Unstable density-driven flow in heterogeneous porous media: A stochastic study of the *Elder* [1967b] "short heater" problem

Awadhesh Prasad and Craig T. Simmons

School of Chemistry, Physics and Earth Sciences, Flinders University of South Australia, Adelaide, South Australia, Australia

Received 7 March 2002; revised 13 May 2002; accepted 15 May 2002; published 16 January 2003.

[1] The situation of a dense fluid overlying a lighter one is potentially unstable and under certain conditions may result in fingers of dense contaminant freely convecting downward. Free convection causes increased contaminant transport over larger distances and over shorter timescales than is possible by diffusion alone. Unlike free convection in homogenous porous media, free convection in heterogeneous porous media has received relatively little attention. In this study, a well-understood problem of transient free convection in homogeneous porous media, the *Elder* [1967b] "short heater" problem has been modified to study the effects of heterogeneity in permeability distributions on solute transport processes using a stochastic framework. A set of measurable indicator characteristics including solute fluxes, solute present, center of gravity and finger penetration depth are used in the quantitative analysis of output. Heterogeneity in the permeability distribution provides both the triggering mechanism for the onset of instabilities and also controls their subsequent growth and/or decay. Results show that (1) an increase in the standard deviation of the log permeability field results in a greater degree of instability at earlier times but promotes stability at later times, (2) an increase in the horizontal correlation length of the log permeability field creates laterally extensive low-permeability zones that dissipate upward and downward motion needed to maintain convection and therefore causes a reduction in the degree of instability, (3) a greater degree of heterogeneity causes greater uncertainty in predictions, and (4) traditional predictive methods such as the Rayleigh number (based upon an average permeability) do not generally work in their application to heterogeneous systems. Probability of exceedence analysis also demonstrates that analyses based upon homogeneous assumptions will typically underestimate, often quite significantly, the value of key measurable characteristics. *INDEX TERMS:* 1829 Hydrology: Groundwater hydrology; 1831 Hydrology: Groundwater quality; 1832 Hydrology: Groundwater transport; 1869 Hydrology: Stochastic processes; *KEYWORDS:* density-driven flow, heterogeneity, free convection, instability, Elder problem

Citation: Prasad, A., and C. T. Simmons, Unstable density-driven flow in heterogeneous porous media: A stochastic study of the *Elder* [1967b] ''short heater'' problem, *Water Resour. Res.*, *39*(1), 1007, doi:10.1029/2002WR001290, 2003.

1. Introduction

[2] Previous field and laboratory studies have shown that fluid density gradients, established by variations in concentration and/or temperature of the fluid, play an important role in solute and heat transport in many groundwater flow systems. Intrusion of seawater in coastal aquifers [*Huyakorn et al.*, 1987], infiltration of leachates from waste disposal sites [*Frind*, 1982], transport of salts due to agricultural practices [*Mulqueen and Kirkham*, 1972] and accumulation and subsequent downward migration of salt near the land surface of a saline lake or playa [*Wooding et al.*, 1997a, 1997b; *Simmons and Narayan*, 1997, 1998] are just a few examples of groundwater systems where fluid density is likely to play an important role in controlling groundwater flow and solute transport processes. Under certain conditions, when a dense fluid overlies a lighter one, free convection driven purely by density differences can occur. This exacerbates the movement of contaminants causing them to move over larger distances within shorter timescales when compared with diffusion. This has important ramifications in the study of contaminant hydrology.

[3] The process of free convection in homogeneous porous media has received considerable attention in the past (for comprehensive reviews on this subject, see *Gebhart et al.* [1988], *Nield and Bejan* [1999], and *Simmons et al.* [2001]). However, free convection in heterogeneous porous media has received considerably less attention. *Schincariol et al.* [1997] studied the effects of heterogeneity (particularly the variance and the correlation length of the random permeability field) on the instability process. They found that increased correlation length scales and increased log permeability variance of the permeability distribution promoted stability. They also suggested that stability criteria that do not incorporate the characteristics of the permeabil-

0043-1397/03/2002WR001290$09.00

ity field would not be suitable for use in natural porous media. In their review paper on variable-density groundwater flow and solute transport in heterogeneous porous media, *Simmons et al.* [2001] carried out numerical experiments to study density-induced instabilities in both periodically structured and random permeability fields. They observed the onset of instabilities and their subsequent growth or decay to be intimately related to both the geometrical structure and the variance of the permeability field. They further noted that stability criteria based upon average statistically equivalent homogeneous properties were inappropriate for describing the onset and propagation of unstable fingers in heterogeneous hydraulic conductivity fields. *Schincariol* [1998] studied the instability of a dense plume in randomly heterogeneous media and noted that even with similar macroscopic field statistics, widely varying degrees of density-induced mixing occur among the different realizations. He concluded that the currently used stability criteria for plume type displacements were not applicable in natural heterogeneous media. These conclusions are consistent with those of *Schincariol et al.* [1997] and *Simmons et al.* [2001].

[4] Although the studies described above have employed random permeability fields, they examine either a single realization or a very small number of realizations. They do not present any statistical analysis of outputs carried out on a larger set of realizations. As we will demonstrate in this study, it is difficult to draw general ''cause and effect'' type conclusions based on dense plume behavior within a single permeability realization as the plume dynamics in another statistically equivalent realization may be entirely different. The effect of heterogeneity in a permeability field on density-induced instability processes may better be quantified through a stochastic analysis of the dense plume problem. This has not previously been attempted and warrants investigation.

[5] In this paper, we present the first systematic stochastic study of free convective processes in heterogeneous porous media using Monte Carlo techniques. The USGS variable-density groundwater flow and solute transport code Saturated Unsaturated, Transport (SUTRA) developed by *Voss* [1984] has been employed. The main objectives of this study are twofold: (1) to quantify the effects of heterogeneity in porous media on density-driven instability processes in order to provide some ''cause and effect'' understanding of trends in system behavior and (2) to quantify the uncertainty in model predictions resulting from the heterogeneity of the media. We have adapted one of the most cited, widely known and well-understood problems of free convection, the *Elder* [1967b] problem to include heterogeneous hydraulic conductivity distributions. The Elder problem was chosen for this study because (1) it is a classical example of free convection phenomena, where bulk fluid is driven purely by density differences, (2) it is a strongly coupled nonlinear problem, (3) the original homogeneous Elder problem (both laboratory and numerically based) is relatively well understood in comparison to many other unstable variable-density flow and transport problems and as a result has become one of the standard benchmarks for ''verifying'' variable-density flow and transport simulators, and (4) it is one of a very limited number of problems that have clearly defined and understood temporal features of unstable plume development (onset of fingers, growth, coalescence etc. . .). Although system geometry and boundary conditions reflect the experimental nature of Elder's original work, the simplicity of this somewhat idealized system offers the advantage of providing an evolving unstable flow system that can be described relatively easily in physical terms and has been previously discussed by numerous authors [e.g., *Voss and Souza*, 1987; *Oldenburg and Pruess*, 1995; *Kolditz et al.*, 1998; *Valliappan et al.*, 1998]. It therefore offers an excellent base case upon which to build a study of the effect of heterogeneity. Results of this study could then form the basis for further analyses that employ different geometry and boundary conditions.

[6] We briefly introduce a set of quantitative indicators or measurable characteristics of instability to describe the instability processes for the homogeneous system (hereafter called the ''base case''). Stochastic results of the heterogeneous adaptation of the Elder problem are then presented and discussed in terms of these indicators of instability.

2. Problem Definition and Methods

2.1. The *Elder* [1967b] "Short Heater" Problem

[7] *Elder* [1967b] presented both experimental and numerical results of thermal convection produced by heating a part of the base of a porous layer. The actual experiment was performed in a Hele-Shaw cell and was called the ''short-heater'' problem. The solute analog of *Elder*'s [1967b] ''short heater'' problem was developed by *Voss and Souza* [1987]. This solute analog (see Figure 1) with identical parameters (Table 1) was used in this study.

[8] The solute source located along the middle half of the top boundary is specified as a constant concentration boundary condition of unit value. The entire bottom boundary is specified as a constant concentration boundary of zero value. Only diffusion (no advection) of solute is possible across the bottom boundary. Initially, the pressure throughout the system is hydrostatic and no solute is present. The solute enters the initially pure water by diffusion increasing fluid density in the boundary layer beneath the source. Free convection begins after sufficient solute accumulation has occurred in the boundary layer.

[9] For ease of comparison, the temporal discretization adopted by *Voss and Souza* [1987] was initially used. A total simulation time of 20 years was discretized into 240 equal time steps each of one month duration. The spatial discretization employed was determined by conducting a grid convergence test using six spatial discretizations: (1) held (61 nodes horizontal (h) $\times$ 31 nodes vertical (v)), (2) peld (81(h) $\times$ 41 (v)), (3) reld (101 (h) $\times$ 41(v)), (4) meld (121(h) $\times$ 31(v)), (5) neld (101 (h) $\times$ 51 (vi)) and (6) teld (121 (h) $\times$ 41 (v)). Of the four finer meshes, the mesh teld with discretization of 121 $\times$ 41 nodes ($\Delta x = 5$ m; $\Delta y = 3.75$ m) was selected because (1) results obtained using this mesh very closely matched those of mesh neld with a higher resolution (101x 51 nodes; $\Delta x = 6$ m; $\Delta y = 3$ m) with the latter consuming more computing time and memory, a particularly important consideration in the Monte Carlo simulation of nonlinear variable-density flow phenomena and (2) the results obtained using this mesh closely matched those of both *Oldenburg and Pruess* [1995] and *Kolditz et al.* [1998] using finer meshes.

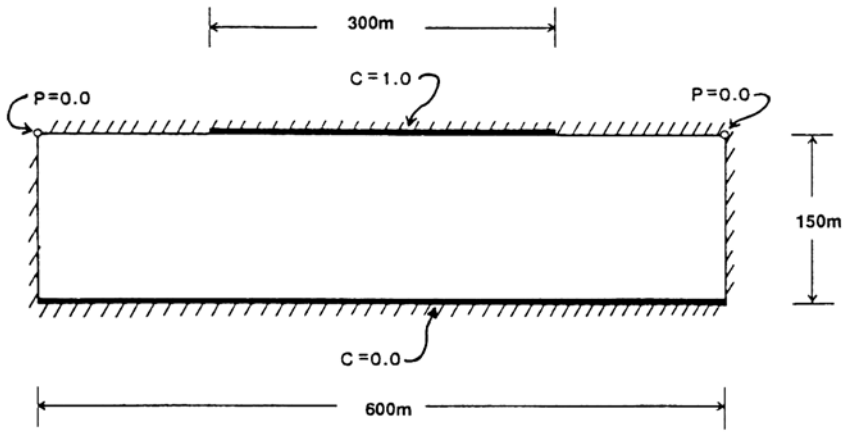

Figure 1. Boundary conditions for the *Elder* [1967b] problem. All boundaries are impermeable. The middle half of the top boundary acts as a solute source and the entire bottom boundary acts as a solute sink. The solute cannot advect across the bottom boundary but can only diffuse through it. Top left and top right nodes are specified pressure of zero. After *Voss and Souza* [1987].

[10] With heterogeneous permeability fields applied to the *Elder* [1967b] problem, the uniform temporal discretization of one month was found to be inadequate at higher standard deviations of the log permeability field ($\sigma_y \geq 0.4$) where a progressively larger number of simulations did not converge. This prompted the use of variable length time steps so as to make the initial time step considerably smaller than one month. An initial time step of one day was chosen with a time step multiplier of 1.5 and time step change cycle of 10. The maximum allowed time step size was one month. The 20 year simulation now had a total of 305 time steps, a factor of 1.3 times greater than that originally used by *Voss and Souza* [1987]. However, even with finer temporal discretization, a very small number of realizations did not converge, when the standard deviation was moderately higher ($\sigma_y \geq 0.5$) owing to the zero longitudinal and transverse dispersivities employed as per the original *Voss and Souza* [1987] adaptation. A compromise was sought between a small modification in the Elder problem on one hand and a significant further refinement of temporal and spatial discretization on the other, with the possibility of a multifold increase in both memory and simulation time requirements. To overcome the problem of nonconvergence for a small number of realizations at higher standard deviations, both longitudinal and transverse dispersivity were increased from 0 to 4.0 meters. This value was obtained through repeated trial and error and examining the number of converged solutions. The lowest value of longitudinal and transverse dispersivity that allowed the solution to converge for all realizations was adopted and is on the order of the element size. After these minor modifications in dispersivity values and time step size, results of the simulation of the Elder problem at different times are given in Figure 2 (left panels). Note that with the modified time step scheme numerical results are now given at 1.02, 2.63, 4.63, 8.63, 10.63, 15.63 and 20.04 years instead of 1, 2, 4, 10, 15 and 20 years. A comparison of results with zero and nonzero dispersivity (Figure 2) show that greater dispersion leads to a wider plume and slightly less distinctive fingering at earlier times. However, the overall nature of instability processes is similar for both cases. Note that the results of the Elder problem with a fine spatial and temporal discretization and a nonzero dispersivity (Figure 2, left panels) closely resemble those of *Voss and Souza* [1987] with a coarse spatial and temporal discretization and zero dispersivities. The simulation with nonzero dispersivities, shown in Figure 2 (left panels), has been adopted as the base case simulation for the stochastic study of dense plume instability in heterogeneous porous media.

2.2. Stochastic (Monte Carlo) Implementation of the Elder Problem

[11] A heterogeneous permeability field characterized by a random spatial function (RSF) is described by three pertinent variables: (1) mean (μ_y), (2) standard deviation (σ_y), and (3) statistical anisotropy, *anis* (the ratio of vertical correlation length (τ_y) to horizontal correlation length (τ_x) of the log permeability field, τ_y/τ_x).

[12] The anisotropy ratio *anis* was controlled by varying the horizontal correlation length. The mesh size and the problem domain size place a restriction on the choice of horizontal correlation length values. The minimum value of horizontal correlation length chosen is 40 m, which contains 8 elements in the horizontal direction ($\Delta x = 5$ m). The vertical correlation length of 30m also contains 8 elements in the vertical direction ($\Delta y = 3.75$ m). The maximum value

Table 1. SUTRA Simulation Parameters for the *Elder* [1967b] Problem[a]

Symbol	Quantity	Value	Units
ε	porosity	0.1	–
C_{INIT}	initial concentration throughout	0.0	kg kg^{-1}
$\partial\rho/\partial C$	coefficient of density variation	200	kg m^{-3}
ρ_0	freshwater density	1000	kg m^{-3}
k	intrinsic permeability	4.845×10^{-13}	m^2
α_L	longitudinal dispersivity	0.0	m
α_T	transverse dispersivity	0.0	m
g	acceleration due to gravity	9.81	ms^{-2}
μ	dynamic viscosity of the fluid	1.0×10^{-3}	kg m^{-1} s^{-1}
D_0	molecular diffusion coefficient	3.565×10^{-6}	m^2 s^{-1}

[a] Parameter values are after *Voss and Souza* [1987].

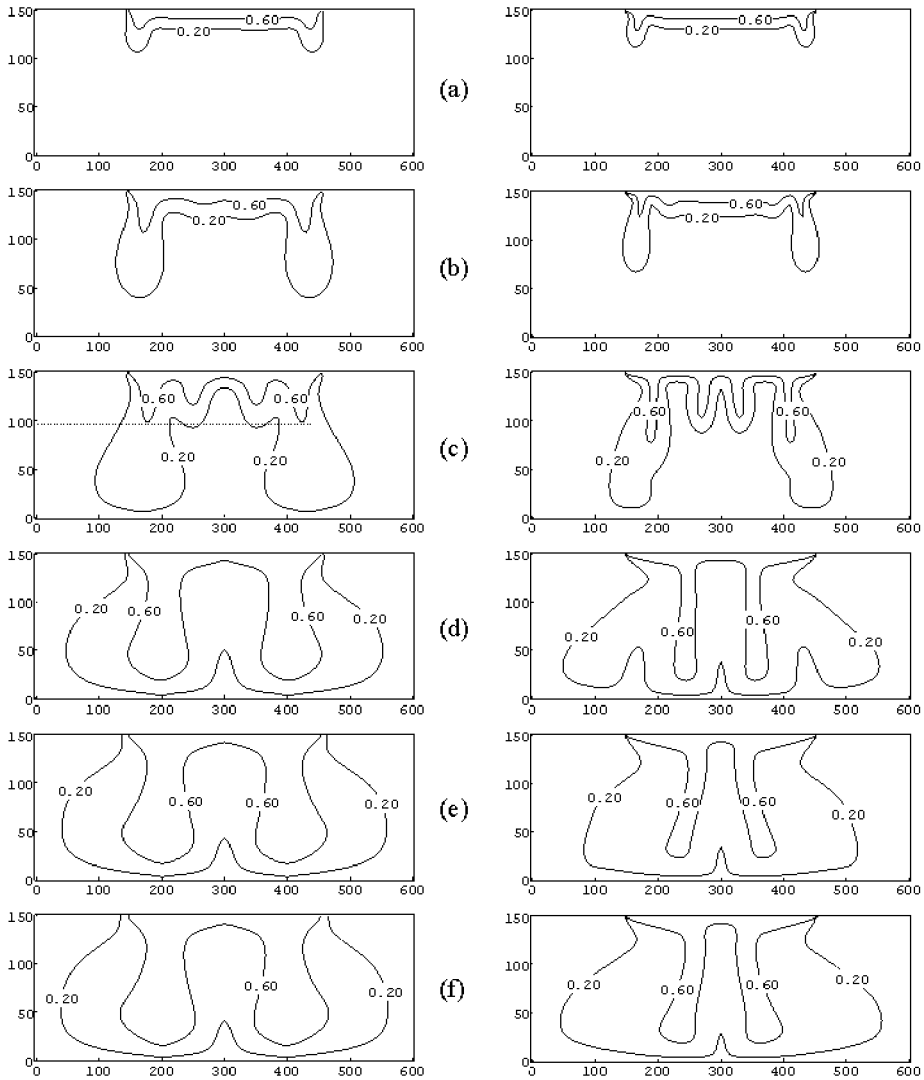

Figure 2. Concentration plots for the Elder problem: modified with nonzero dispersivity (left panels) at elapsed times of (a) 1.02 years, (b) 2.63 years, (c) 4.63 years, (d) 10.63 years, (e) 15.63 years, and (f) 20.04 years and for the original problem with zero dispersivity (right panels) at elapsed times of (a) 1 year, (b) 2 years, (c) 4 years, (d) 10 years, (e) 15 years, and (f) 20 years. Both longitudinal and transverse dispersivities for the modified problem have been set at 4 m instead of zero as in the original *Elder* [1967b] problem adapted by *Voss and Souza* [1987] for the solute transport. The penetration depth of the 0.6 contour at 4.63 years (Figure 2c, left) is just greater than 50 m.

of horizontal correlation length has been restricted to 150 m, so that the field will have at least 4 correlation lengths in the horizontal direction (L = 600 m). These restrictions on minimum and maximum value of correlation lengths were used to preserve realization statistics, i.e., to ensure that the statistical properties of all realizations within a set of simulations remain constant throughout.

[13] The Sequential Gaussian Simulation (*SGSIM*) method of GSLIB [*Deutsch and Journel*, 1992] with an exponential variogram was used to generate random permeability fields which were then applied the *Elder* [1967b] problem. Thirty Monte Carlo (*MC*) simulations were run for each set of identical input variables giving a confidence interval of $\pm 0.36\sigma$ at a confidence level of 95% [*Kreyszig*, 1988]. Thus on 95% of occasions the mean values of the output variables will lie within $\pm 0.36\sigma$. Four experimental series were examined: (1) variation of σ_y at constant μ_y (-12.315) and *anis* (0.3) series (σ_y = 0.1, 0.2, 0.4, 0.5, 0.6), (2) variation of τ_x series (τ_x = 40 m, 80 m, 100 m, 120 m, 150 m) at constant σ_y (0.4) and μ_y (-12.315), (3) μ_y series (μ_y = -12.315, -12.917, -13.315, -13.917, -14.917) at constant σ_y (0.4) and *anis* (0.3) and (4) variation of σ_y at a lower μ_y (-13.917) and *anis* (0.3) series (to examine a larger range of σ_y = 0.2, 0.4, 0.8, 1.2, and 1.4, μ_y was lowered to eliminate the problem of nonconvergence at the higher μ_y).

2.3. Generation of Instabilities

[14] When density variations (where a dense fluid overlies a less dense one) within a fluid body are significant, solute transport may be the result not only of forced

(hydraulically driven) convection (also commonly called advection) but also of free convection [*Gebart et al.*, 1988]. If the density difference is sufficiently high, free convection can occur and an instability forms in which lobes of dense fluid move downward counterbalanced by less dense fluid moving upward. It is the density stratification that is the main cause of the instability process which causes the fluids to mix to achieve a stable density gradient [*Schincariol and Schwartz*, 1990]. In flow through a porous medium, perturbations or interfacial disturbances are continuously generated because of heterogeneities in the medium [*Moissis and Wheeler*, 1990]. These perturbations to flow occur on many spatial scales ranging from pore scale heterogeneities to much larger heterogeneities on the scale of the problem under consideration. Whether or not these perturbations become unstable depends upon whether their wavelength exceeds some critical wavelength, which is a function of flow and transport parameters [*Schincariol et al.*, 1994].

[15] *Schincariol et al.* [1994] also pointed out that numerical errors in solute transport codes may serve as a perturbing function and lead to the development of instabilities in a variable-density flow system. In numerical model simulations such instabilities may not be realistic and are usually uncontrollable. Furthermore, coarse discretization can lead to significant numerical errors and numerical dispersion that can alter the shape and growth of developing fingers once they are generated. To overcome problems associated with uncontrolled numerical perturbations to flow and numerical dispersion effects, it is necessary to use fine spatial and temporal discretization in the numerical solution. It is expected and observed that in the simulation of dense plume migration in heterogeneous porous media that the variability in hydraulic properties is significantly more important in controlling where instabilities form, their initial flow rates, their evolving spatial distribution with time as well as macroscopic dispersive mixing associated with transport.

2.4. Measurable Characteristics of Instability

[16] In order to quantify whether or not instability is expected to, or does, occur it is necessary to identify a number of measurable characteristics. A traditional predictor of instability is the dimensionless Rayleigh number (*Ra*) defined as a ratio of buoyancy driven flux to diffusive flux given by

$$Ra = \frac{\text{Buoyancy/Gravitational flux}}{\text{Diffusive/Dispersive flux}} = \frac{gk\beta\Delta CH}{\varepsilon\nu_0 D_0} \qquad (1)$$

where g is acceleration due to gravity, k is the intrinsic permeability, $\beta = \rho_0^{-1}(\partial\rho/\partial C)$ is the linear expansion coefficient of fluid density with changing fluid concentration, ΔC is the concentration difference between high- and low-density fluids, H is depth of the porous layer, ε is the aquifer porosity, ν_0 is the kinematic viscosity of the fluid and D_0 is the molecular diffusivity.

[17] The input parameters (see Table 1) that define the *Elder* [1967b] problem result in a value of $Ra = 400$. The critical Rayleigh number (the minimum value of the Rayleigh number at which instability occurs) for the Elder problem is 40 [*Elder*, 1967a]. On this basis, convection would be expected to occur in the flow system studied by *Elder* [1967a, 1967b].

[18] We use the following set of measurable characteristics in this study to assess system behavior as being either stable or unstable and in the statistical analysis of simulation output: (1) Concentration distribution (expressed as a dimensionless mass fraction) of the solute in the aquifer at any time for visual evidence of fingering. (2) Nusselt number: the dimensionless Nusselt number (*Nu*) is defined as the ratio of actual mass transfer rate when free convection is present to the steady state mass transfer rate due to diffusion alone given by

$$Nu = \frac{\text{Actual mass flux}}{\text{Diffusive mass flux}} = \frac{QH}{WL_s D_0 \Delta C} \qquad (2)$$

where Q is the solute flux across the boundary and W and L_s are the width and length of the source boundary respectively. Since the Nusselt number is a dimensionless representation of solute flux across a source boundary, it is small for diffusive systems and significantly larger in systems where unstable convection dominates transport. (3) Solute present (*SP*): This quantity is proportional to the amount of solute present in the aquifer at any time and is calculated by finding the area under the average concentration (at any given depth) versus depth graph. It is the amount of solute mass present in the aquifer per unit cross-sectional area per unit coefficient of density change ($\partial\rho/\partial C$). The dimension of *SP* obtained by computing the area under the average (dimensionless) concentration versus depth curve is (m). (4) Center of gravity of the plume (*CGP*): This quantity is the vertical center of the gravity of the plume present in the aquifer at any time measured from the source boundary. In a free convective system processes in the vertical direction dominate flow and transport. The depth of plume migration in the (vertical) direction of gravity is an important indicator of instability. Horizontal movement could also be quantified in a heterogeneous system given that resultant plumes are typically nonsymmetric. However, in considering whether behavior is stable or unstable, horizontal movement is a significantly less sensitive indicator than vertical movement. In other systems that employ different geometries, boundary conditions or a horizontal ambient flow, some measure of lateral movement may also be important. First, second or third plume moments could be used in such cases. (5) Penetration depth (*PD*): This quantity is the maximum penetration depth of the 0.6 contour measured from the top boundary. Though it is possible to monitor any concentration level, we have selected the 0.6 contour as it is traditionally used in presenting concentration solutions for the Elder problem.

[19] Interestingly, there is a wide range of other indicator variables that could be employed in such a study and as such, the measurable characteristics employed here are by no means complete. Others that could be used to indicate the presence of unstable behavior might include the maximum velocity of the plume with time, evidence of fluid circulation in velocity vector fields and the spatial distribution of solute transfer across the source boundary. These are not considered here.

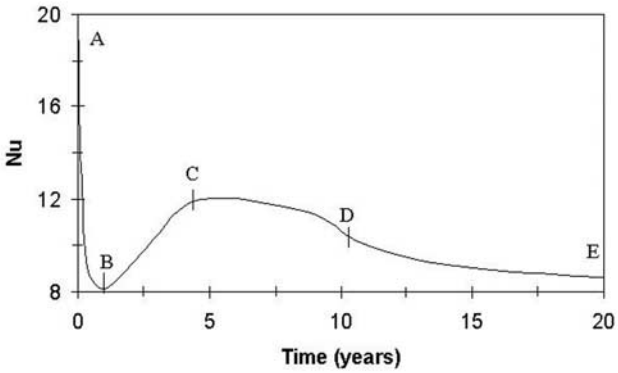

Figure 3. Nusselt number versus time (years) curve for the homogeneous (base) case showing different stages of instability. The boundary layer forms between *A* and *B*. *B* is the point of onset of instability. *C* is the point when the plume first touches the bottom. At *D* the denser portion of the plume reaches the bottom in the interior. Between *D* and *E* only diffusive spreading takes place.

[20] Results for some of these indicator variables are given for the homogeneous Elder problem (base case) in Figure 2 (concentration distribution), Figure 3 (*Nu*), and Figure 4 (*SP*, *CGP*, and *PD*). These results clearly illustrate how these variables can be applied to help explain various aspects of the instability problem. A brief description of these results is now given. In Figure 3, the changes in *Nu* with time mark four distinct solute transport regimes. Initially solute enters the system through diffusion. At early times, vertical concentration gradients at the top boundary are very high so that the rate of solute transfer is correspondingly high. As the solute enters the aquifer, vertical concentration gradients are reduced near the source and consequently the rate of solute transfer is reduced. This reduction in *Nu* continues until about one year. By this time, sufficient solute has accumulated in the top boundary layer beneath the source to cause instability (Figure 2, left panels). Growth of fingers due to gravitational instability begins and is accompanied by an increase in solute transport (Figure 3). When compared with the concentration plot shown in Figure 2 (left panels), it can be seen that the growth of the 0.6 contour is retarded between about 3 and 5 years. This is because the 0.6 contour is unable to penetrate any further due to a reduction in the concentration gradient within the outer edge fingers. During this period instability activity shifts to newly developing inner fingers which now begin to grow. Because finger growth is now divided among a greater number of fingers, the *PD* curve (Figure 4) shows a significant reduction in growth rate between about 3 and 5 years. In this period, growth of already established outer fingers almost stagnates as developing internal fingers grow and consequently *Nu* continues to increase. The increase in *Nu* continues until about 5 years when the lighter portion of the plume touches the bottom. Because the plume has reached the bottom, the vertical concentration gradient within the plume is reduced as solute begins to accumulate above the bottom boundary. Although fingers continue growing in that the heavier portion of the plume continues to sink (at reduced rates), the mass transfer rate is slowed down due to the reduction in concentration gradients which are progressively felt closer to the source as mass accumulation continues. Beyond about 5 years, coalescence of fingers occurs and outer edge fingers continue to move downward after entrainment of interior fingers and an increase in the growth rate of the 0.6 contour is observed. By about 9 years, the bulk of the plume has reached the bottom. The plume now spreads laterally by diffusion and dispersion. There is almost no further increase in *PD* after this time. There is a sharp decrease in the solute transport rate because fingers cannot grow further. The increase in *SP* is almost linear up to around 9 years which indicates the dominance of free convection (instability) as the main solute transport mechanism. After this time, the growth of *SP* slows as the plume has now touched the bottom. Similar arguments as given for *SP* and *PD* indicator variables explain the trend in *CGP* with time and will not be repeated here.

3. Results and Discussion

[21] We begin by presenting a preliminary assessment of the heterogeneous adaptation of the Elder problem by way of visual inspection and describe why a stochastic analysis of the problem is warranted. The effect of each of the input variables (standard deviation, correlation length and mean of the permeability distribution) on measurable output indicators is then described within a stochastic framework. In each case, the key observation made is the variation of both the mean and standard deviation of each output variable with time. In light of these results, we discuss the limitations of the use of the traditional Rayleigh number in its ability to predict the onset of instability in heterogeneous systems. A probability of exceedance analysis is then presented to demonstrate the implications of assuming homogeneous conditions apply when heterogeneous conditions actually exist. Finally, the variation of correlation coefficients between output indicators with time is examined to demonstrate why numerous measurable characteristics of instability may be desirable in the study of dense plume migration in heterogeneous porous media.

3.1. A Preliminary Assessment

[22] We begin by a visual inspection of some results of the heterogeneous Elder problem. Figure 5 shows the

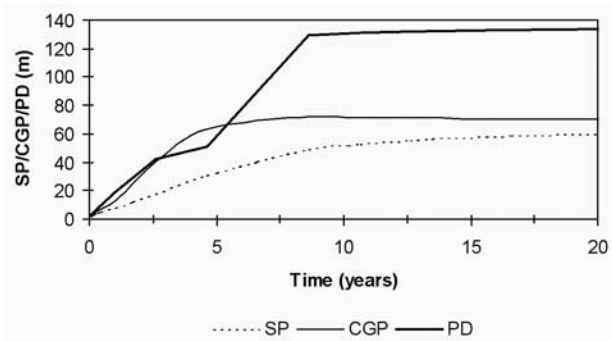

Figure 4. The solute present (SP), the center of gravity of the plume (CGP), and penetration depth (PD) of 0.6 contour versus time for the homogeneous (base) case.

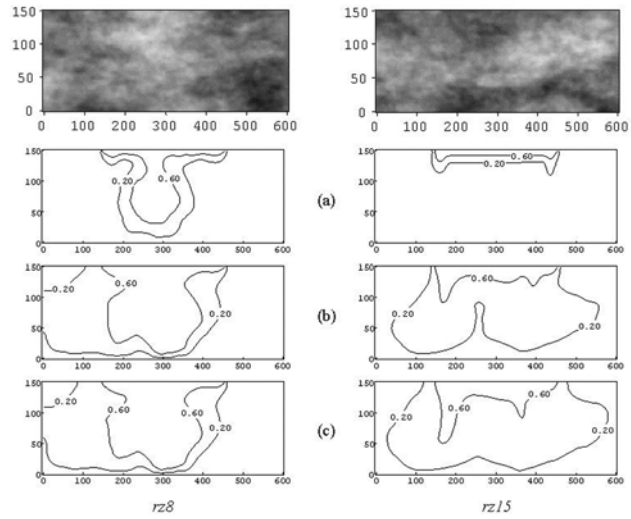

Figure 5. Concentration plots for two statistically equivalent random permeability fields (shown at top where darker regions correspond to areas of lower permeabilities, and lighter regions correspond to areas of higher permeabilities), *rz8* (left panels) and *rz15* (right panels) at elapsed times of (a) 1.02 years, (b) 10.63 years, and (c) 20.04 years. These two fields are from the same simulation set, *rg3sd4* with identical statistical parameters ($\mu_y = -12.315$; $\sigma_y = 0.6$; $\tau_x = 100$ m and *anis* = 0.3).

concentration plots at simulation times: (1) 1.04, (2) 10.63 and (3) 20 years for two arbitrarily selected realizations, *rz8* and *rz15* from the simulation set *rg3sd4* all of which have identical statistics ($\mu_y = -12.315$; $\sigma_y = 0.6$; $\tau_x = 100$ m and *anis* = 0.3). The resulting fields have an average permeability of 4.845×10^{-13} m^2 which is equal to the permeability value used in the simulation of the original homogeneous (base case) Elder problem. It is clear from Figure 5 that the temporal and spatial response of these two statistically equivalent fields are significantly different. An inspection of the permeability distributions also shown in Figure 5 suggests that solute transport processes are very sensitive to the locations of high- and low-permeability zones especially near the top boundary. This inherent difference among the response of different realizations is the fundamental reason for undertaking a stochastic analysis of the dense plume problem.

[23] Having established that two statistically equivalent fields result in significantly different behavior of the propagation of an unstable plume, the next question to explore is what the effect of change in the heterogeneity (σ_y) of the permeability distribution is on the instability process. We do this by varying σ_y (0.1, 0.2, 0.4, 0.5, 0.6) in these two fields while keeping all other parameters constant. The effect of the variation in σ_y of these two sets of fields, *rz8* and *rz15* is shown in Figure 6 as concentration plots at a simulation time of 10.63 years (responses for three values of $\sigma_y = 0.1$, 0.4, 0.6 are shown in addition to the homogeneous case). The responses of realization set *rz15* (Figure 6, right panels) shows that an increase in degree of heterogeneity amplitude (i.e., increase in σ_y) tends to dissipate fingers by dispersive mixing (note the variation in the penetration depth of the 0.6 contour) and therefore reduces the degree of instability. *Schincariol et al.* [1997] and *Schincariol* [1998] arrived at the same conclusion in their deterministic study. But will an increase in the degree of the heterogeneity (σ_y) always promote stability? An observation of plume dynamics in the field *rz8* (left panels) in Figure 6 shows that an increase in the degree of the heterogeneity appears to have enhanced the degree of instability.

[24] To further explore the effect of heterogeneity on the range of likely behavior, both the maxima and minima of output variables *Nu*, *SP*, *CGP*, and *PD* within a set were identified and plotted against time (Figure 7) after analysis of two complete simulation sets, *rg3sd1* ($\sigma_y = 0.1$) and *rg3sd4* ($\sigma_y = 0.6$). It is seen in Figure 7 that the maxima of all these output variables for any time step corresponding to the simulation set *rg3sd1* ($\sigma_y = 0.1$) are greater than the minima of all output variables for the simulation set *rg3sd4* ($\sigma_y = 0.6$). This suggests that although σ_y of simulation set *rg3sd4* is greater than σ_y of simulation set *rg3d1*, there are some realizations in simulation set *rg3sd4* for which the minimum value of any output variable is lower than the maximum value of that output variable for some realizations in simulation set *rg3sd1*. Thus increasing σ_y does not always reduce the degree of instability and clearly a range of behavior is observed. The deterministic conclusion that increasing σ_y will necessarily result in a decrease or an increase in the degree of instability is therefore not valid and a stochastic analysis is warranted.

3.2. Effect of σ_y on Output Variables

3.2.1. Concentration Distributions

[25] Figure 8 shows the effect of σ_y on the mean concentration distribution at two elapsed simulation times 2.63 and 15.63 years (mean concentration profiles pertaining to three values of $\sigma_y = 0.1$, 0.4 and 0.6 are shown in addition to the homogeneous case $\sigma_y = 0$). When the degree of heterogeneity is small (i.e., $\sigma_y \rightarrow 0$) the ''mean'' system behavior approaches that of the homogeneous case. As σ_y increases, the deviation of the mean concentration profile from the homogeneous case becomes significant. At earlier times, an increase in σ_y creates preferential flow paths that cause enhanced fingering as evidenced by an additional central finger. However, at later times greater σ_y is associated with subdued fingering where increased heterogeneity is responsible for finger ''smearing'' as a result of greater dispersive mixing.

[26] Figure 9 shows the effect of various σ_y on the standard deviation of concentration distribution at simulation times of 2.63 and 15.63 years. It is seen that as σ_y increases the standard deviation of the concentration field also increases (as observed by the increasing areas enclosed by different contour levels). An interesting observation is that the uncertainty in the concentration field is typically higher in the middle of the plume than at its edges. This is explained by the fact that fingers, which develop more easily at outer boundary edges [*Wooding et al.*, 1997a, 1997b; *Simmons et al.*, 1999] are dominant and persistent. These fingers are present in most cases and are typically able to overcome the permeability distribution provided that the permeability in their vicinity is not too low. Conversely, internal fingers may be present in some conducive realizations and not in others. Hence, greater variability in finger-

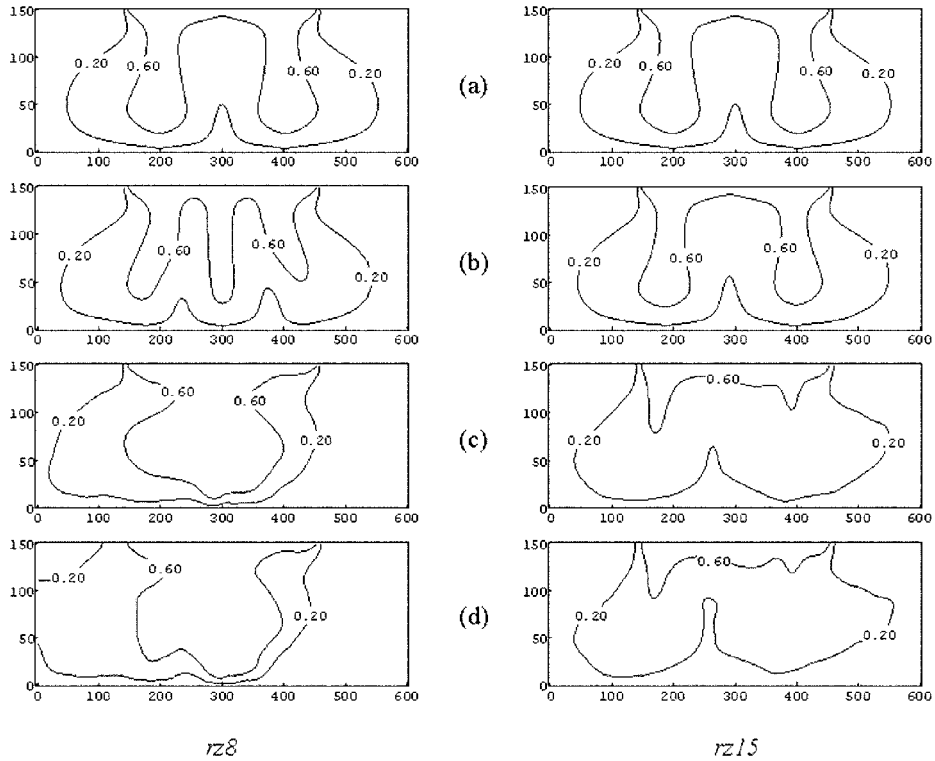

Figure 6. Concentration plots at elapsed time 10.63 years for realizations *rz8* (left panels) and *rz15* (right panels) with standard deviations of (a) $\sigma_y = 0$ (homogeneous), (b) $\sigma_y = 0.1$, (c) $\sigma_y = 0.4$, and (d) $\sigma_y = 0.6$. Corresponding permeability fields have identical $\mu_y = -12.315$; $\tau_x = 100$ m and *anis* = 0.3.

ing occurs in the interior of the plume than at its outer edges.

3.2.2. Nusselt Number (Nu)

[27] Figure 10a shows the effect of σ_y on the mean Nusselt number (μ_{Nu}). It is seen that μ_{Nu} increases with increasing σ_y until about 5 years (the time it takes in the homogeneous case and for the "mean" plume in heterogeneous case to reach the bottom of the system). Beyond this time, μ_{Nu} decreases with increasing σ_y. Increasing the degree of heterogeneity provides a greater opportunity for preferential flow. Initially the degree of instability is greater with larger σ_y and thus an increase in μ_{Nu} is noted (the

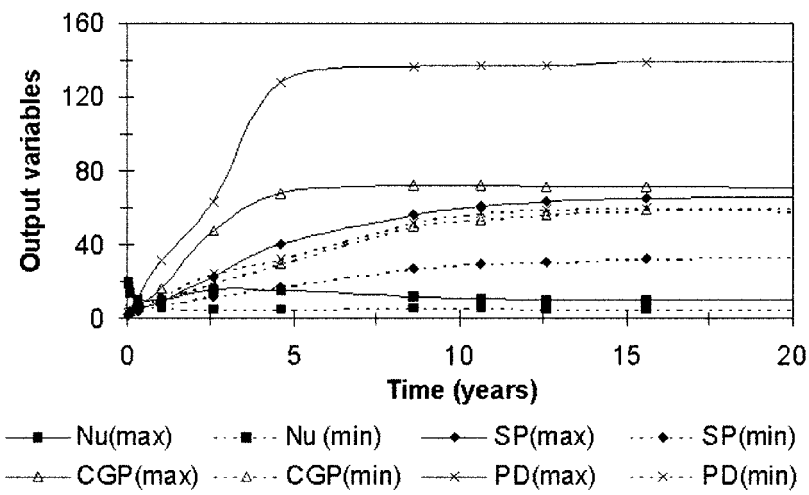

Figure 7. The time variation of output variables: the maxima for the simuation set *rg3sd1* ($\sigma_y = 0.1$) and the minima of the simulation set *rg3sd4* ($\sigma_y = 0.6$). Solid lines represent maxima, and dashed lines represent minima. The maxima of all variables of set *rg3sd1* (lower σ_y) are always greater than the corresponding minima of the set *rg3sd4* (higher σ_y). The mean ($\mu_y = -12.315$) and the correlation length ($\tau_x = 100$ m) are constant for both sets.

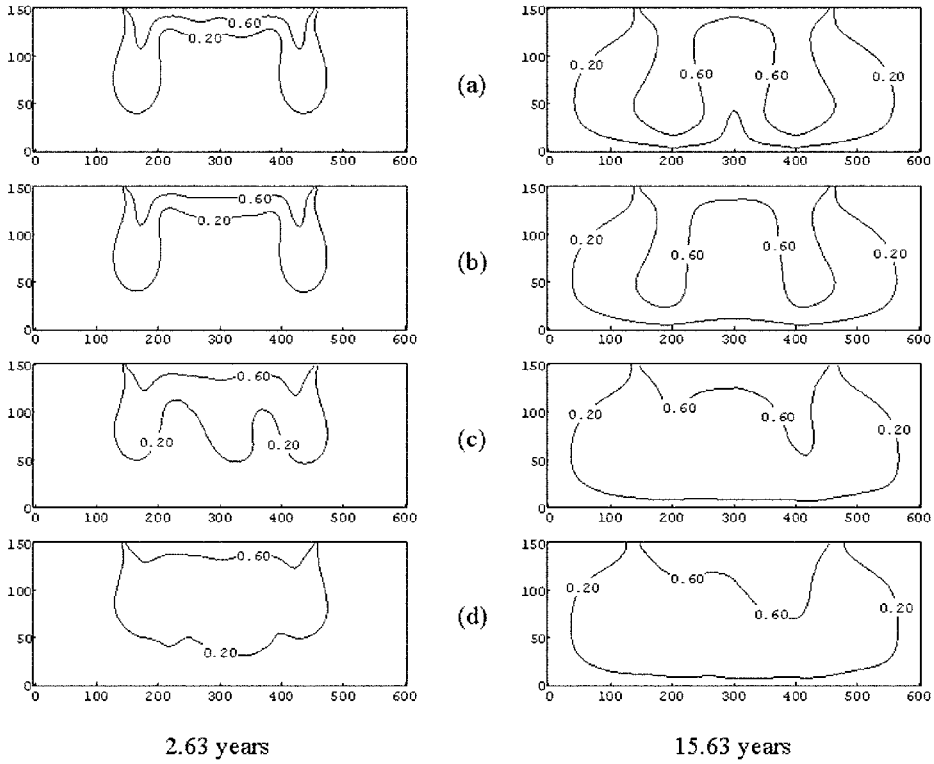

Figure 8. Mean concentration plots at elapsed times of 2.63 years (left panels) and 15.63 years (right panels) for standard deviations of (a) $\sigma_y = 0$ (homogeneous), (b) $\sigma_y = 0.1$, (c) $\sigma_y = 0.4$, and (d) $\sigma_y = 0.6$. Higher σ_y gives rise to significant departure from the homogenous concentration distribution.

homogeneous case gives the lowest μ_{Nu} at the minima). However, at later times increased heterogeneity promotes dispersive mixing and causes a reduction in μ_{Nu}. The homogeneous system is therefore able to maintain higher solute fluxes than is typical for the heterogeneous realizations.

[28] It is observed from the σ_{Nu} versus time graph in Figure 10b that an increase in σ_y always results in an

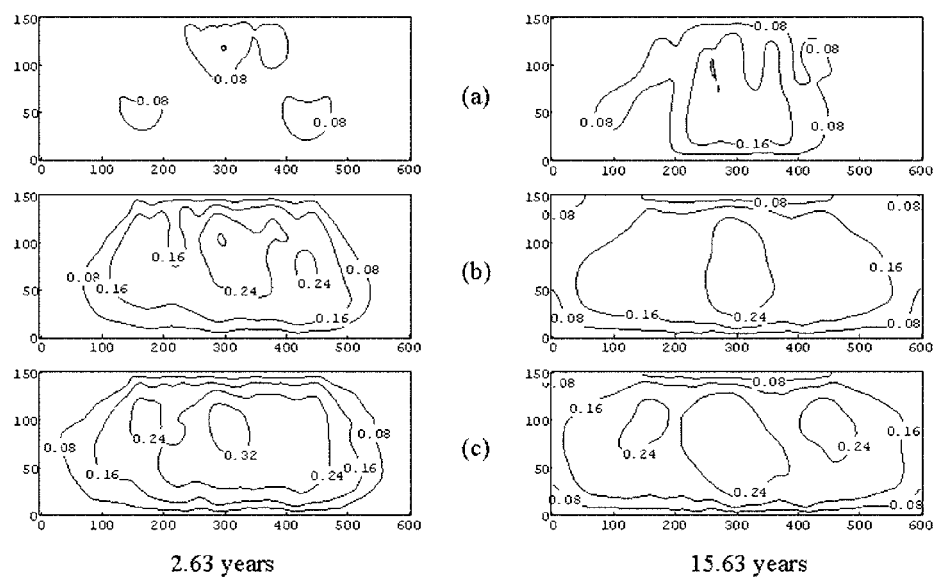

Figure 9. Contour plots of standard deviations of the concentration field at elapsed times 2.63 years (left panels) and 15.63 years (right panels) for standard deviations of (a) $\sigma_y = 0.1$, (b) $\sigma_y = 0.4$, and (c) $\sigma_y = 0.6$. Standard deviations of the concentration field are higher in the interior and lower at exterior of the plume and increase with increasing standard deviations (of log k), σ_y.

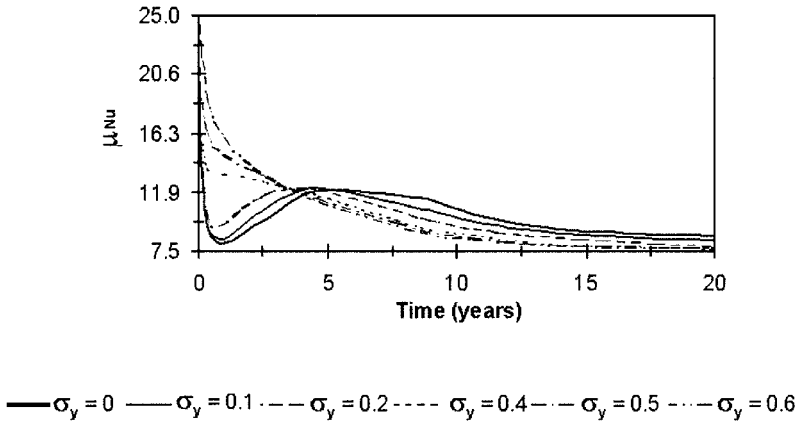

(a)

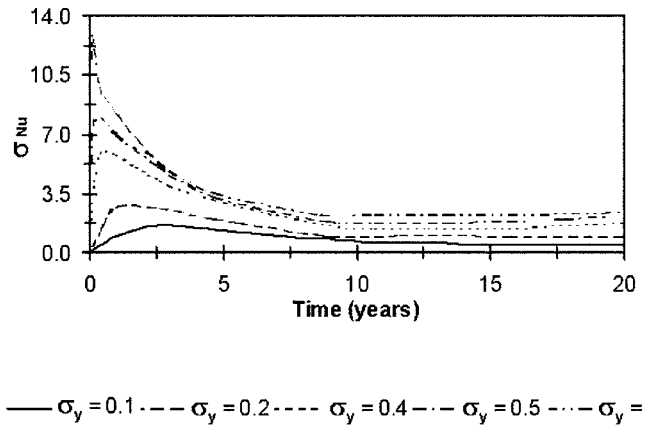

(b)

Figure 10. Variation of (a) the mean of the Nusselt number μ_{Nu} and (b) the standard deviation of the Nusselt number σ_{Nu} with time for different values of standard deviation (of log k) σ_y.

increase in σ_{Nu}. For any degree of heterogeneity (σ_y) some realizations may be highly conducive to instability, while others may be moderately conducive or even unconducive, depending upon the local distribution of high- and low-permeability zones near the upper (solute source) boundary. Thus differences in *Nu* responses of individual fields will be higher for higher values of σ_y and vice versa. This explains the increase inσ_{Nu} with increasing σ_y.

[29] The temporal variation of σ_{Nu} in Figure 10b shows two interesting features: (1) σ_{Nu} increases with time to reach a maximum and then decreases and (2) as σ_y increases, the time at which the maximum in σ_{Nu} is observed is correspondingly earlier (for σ_y = 0.1 the maximum value of σ_{Nu} occurs at about 3 years, whereas for σ_y = 0.6, the maximum value of σ_{Nu} occurs at about 0.1 years). This can be explained as follows. Initially all realizations are at the same state. With increasing time, some of the more conducive realizations become unstable and experience higher values of *Nu*, while others are relatively more (or completely) stable in their behavior. Thus the process of instability causes differences in response among the individual realizations. The instability grows with time until it reaches a maximum. As concentration gradients are reduced within the flow system the instability process is then dissipated by dispersive/diffusive processes. The gradual return to stability at later times reduces the solute flux across the upper boundary and the difference among realizations (with respect to *Nu*) is consequently reduced. Hence σ_{Nu} increases with time, reaches a maximum and then decreases. With larger σ_y, greater differences in *Nu* responses occur and also occur correspondingly earlier owing to the earlier onset of instability in the more conducive realizations. However, the decay/mixing process also sets in earlier. This causes maxima in σ_{Nu} to occur progressively earlier with time for increasing values of σ_y.

3.2.3. Solute Present (SP)

[30] Figure 11a depicts the effect of σ_y on μ_{SP}. It is seen that increasing σ_y causes an increase in μ_{SP}. This increase in μ_{SP} due to an increase in σ_y continues until about 10 years.

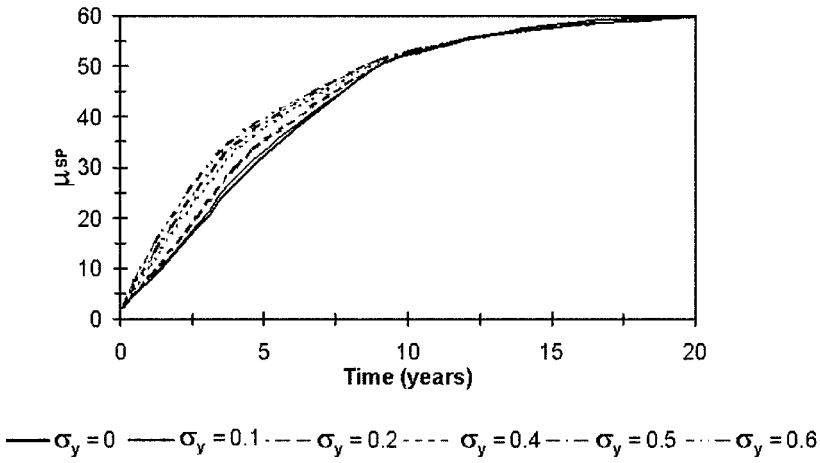

(a)

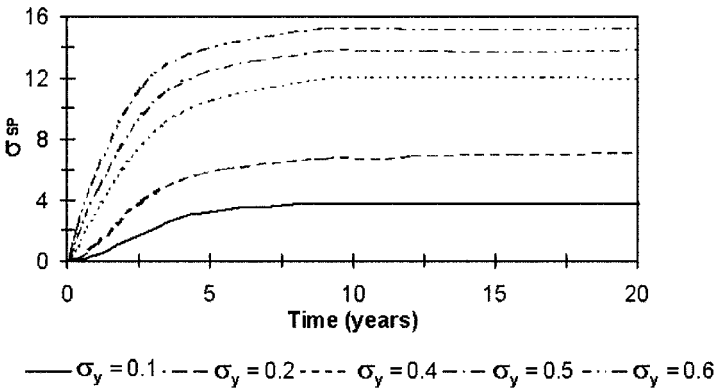

(b)

Figure 11. Variation of (a) the mean of the solute present μ_{SP} and (b) the standard deviation of the solute present σ_{SP} with time for different values of standard deviation (of log k) σ_y.

Beyond this time, there is little change in μ_{SP} with increasing σ_y. Higher σ_y results in a higher degree of initial instability and thus higher σ_y is associated with higher μ_{SP}. As time passes the aquifer progressively fills with solute. Thus at later times all systems with different σ_y approach similar values of μ_{SP} with the contrast between realizations progressively diminishing. At later times there is little, if any, impact on μ_{SP} caused by σ_y.

[31] The effect of σ_y on σ_{SP} is shown in Figure 11b. There are two main observations here: (1) an increase in σ_y causes an increase in σ_{SP} and (2) σ_{SP} increases with time and attains a constant value around 9 years. An increase in σ_{SP} is expected to occur with an increase in σ_y. However, a direct plot of σ_{SP} with σ_y would show a near linear increase in σ_{SP} with increasing σ_y. One possible reason for this behavior is that because *SP* is a space averaged variable, the uncertainty (σ_y) in the input is linearly transferred to the uncertainty (σ_{SP}) in the output. The temporal variation of σ_{SP} is explained as follows. Initially differences among individual responses increase because of the increasing difference between the rate of solute accumulation in two groups of realizations: (1) high rates of solute accumulation in highly conducive realizations and (2) low rates of solute accumulation in less conducive realizations. This continues until around 9 years. Therefore, σ_{SP} increases until around 9 years. The difference among the responses of individual realizations becomes constant by about this time. The most plausible explanation for this behavior is that unstable realizations have similar solute contents (*SP*), as they are almost filled up; while those not so conducive realizations also have similar (but significantly lower than the former) solute contents (*SP*) due to very slow mass accumulation in

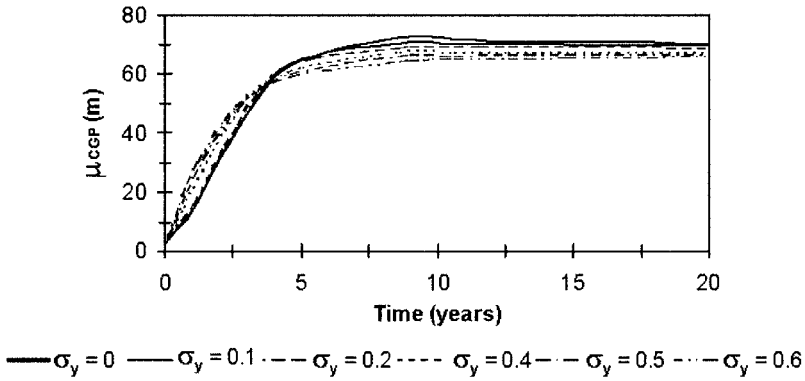

(a)

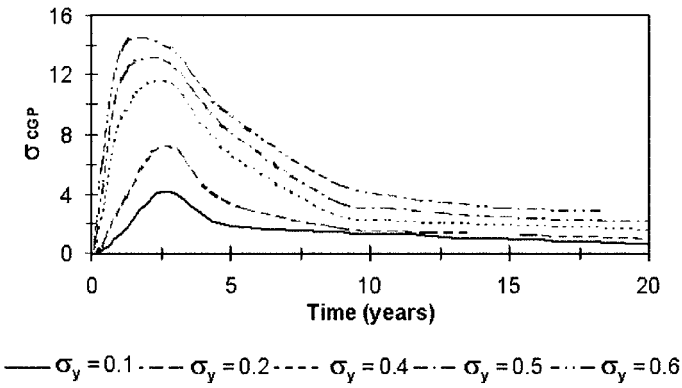

(b)

Figure 12. Variation of (a) the mean of the center of gravity of the plume μ_{CGP} and (b) the standard deviation of the center of gravity of the plume σ_{CGP} with time for different values of standard deviation (of log k) σ_y.

them. Thus the difference between two groups (at later times) is a difference between two states: the extensively penetrated plumes which have reached the bottom and the stable plumes that do not move far from the top boundary. These two states do not significantly change with increasing time. Thus σ_{SP} stabilizes at around 9 years.

3.2.4. Center of Gravity of the Plume (CGP)

[32] Figure 12a shows the effect of σ_y on μ_{CGP}. It is observed from this figure that an increase in heterogeneity causes: (1) an increase in μ_{CGP} at times earlier than about 5 years and (2) a decrease in μ_{CGP} at later times. At earlier times, the higher degree of heterogeneity causes a higher degree of fingering instabilities due to the presence of larger preferential flow paths. This causes a greater downward movement of mass. This explains why a higher degree of heterogeneity causes an increase in μ_{CGP} at earlier times. However, an increase in the degree of heterogeneity (σ_y) as explained earlier, promotes spreading and dispersive mixing at later times. Because of this spreading, concentration gradients are reduced and the growth of μ_{CGP} with an increase in σ_y is retarded. Thus larger σ_y results in smaller μ_{CGP} growth at later times. A slight decrease is observed in μ_{CGP} for the homogeneous and mildly heterogeneous systems at later times. In these systems, μ_{CGP} has already reached a maximum value as the heavier portion of the plume has already touched the bottom. When mass continues to build up in the plume, it will accumulate on the top of the mass already present, thereby pushing *CGP* back upwards. Thus μ_{CGP} is slightly reduced. On the other hand, μ_{CGP} continues to increase with time in the case of a highly heterogeneous system, albeit very slowly because μ_{CGP} has not yet reached a maximum.

[33] Figure 12b shows the effect of σ_y on σ_{CGP}. Two main observations here are (1) an increase in σ_y causes an increase in σ_{CGP} and (2) σ_{CGP} first increases with time, reaches a maximum and then starts decreasing for all values of σ_y. The larger σ_{CGP} associated with increasing σ_y is due to the greater contrast between *CGP* responses among

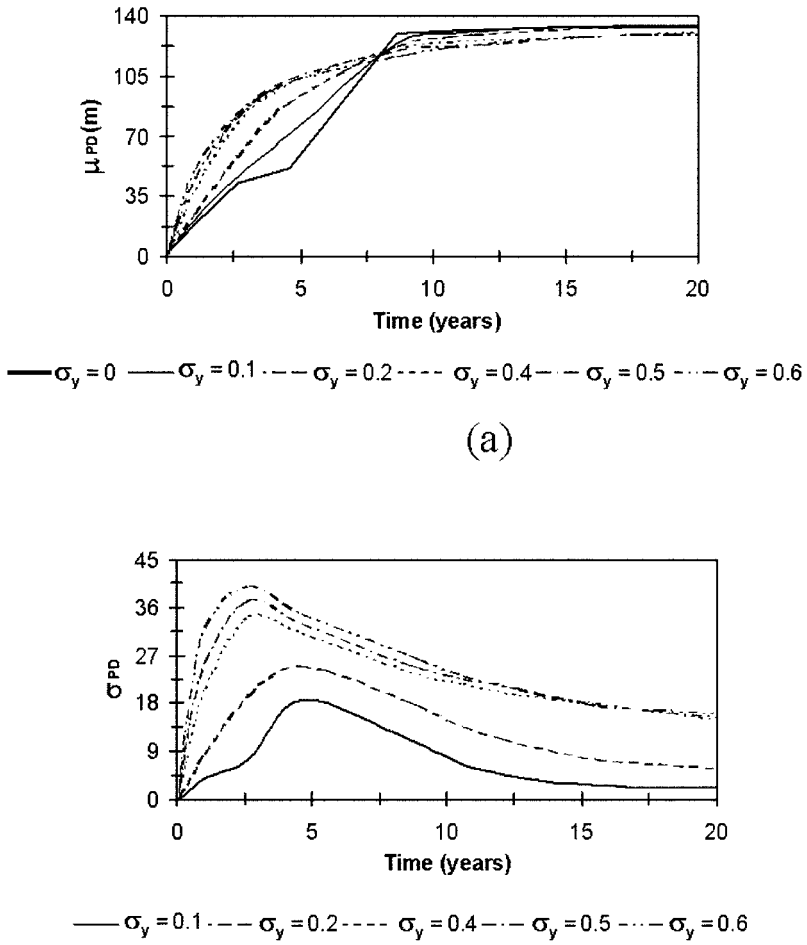

Figure 13. Variation of (a) the mean of the penetration depth (of 0.6 contour) μ_{PD} and (b) the standard deviation of the penetration depth (of 0.6 contour) σ_{PD} with time for different values of standard deviation (of log k) σ_y.

different realizations. The temporal variation of σ_{CGP} is explained as follows. It has been observed and previously discussed that an increase in σ_y increases the degree of instability in conducive realizations at earlier times. This means that individual differences in *CGP* are higher at early times hence the growth rate of σ_{CGP} is higher at earlier times. At later times, systems begin to stabilize and the associated uncertainty reduces. Thus the rate of growth of σ_{CGP} reduces and a plateau in the graph is observed.

3.2.5. Penetration Depth of the 0.6 Contour (PD)

[34] Figure 13a shows the relationship between σ_y and μ_{PD}. It is observed from Figure 13 that an increase in σ_y causes an increase in μ_{PD} at times earlier than 9 years and a decrease in μ_{PD} at later times. Higher σ_y means that the contrast between the lower permeability and higher permeability zones is greater. Due to this contrast, the existence and the growth of an isolated deep finger is more likely to occur in a heterogeneous system than a homogeneous one at earlier times. At later times, heterogeneity promotes dispersive mixing which explains the reduction in μ_{PD} with increasing σ_y. An interesting feature of Figure 13a is that as σ_y increases the curve becomes steeper, showing very high initial growth and a later flattening compared to the homogeneous case. This is because on average highly heterogeneous systems are more unstable initially than less heterogeneous ones. It is again consistent with earlier observations of the other instability indicators.

[35] The effect of σ_y on σ_{PD} in Figure 13b shows that (1) an increase in σ_y causes an increase in σ_{PD}, (2) σ_{PD} increases with time, reaches a maximum then decreases, and (3) the time at which the maximum in each case occurs is correspondingly earlier with increasing σ_y. It is also observed that σ_{PD} is not a linear function of σ_y. Linearity should not be expected here because *PD* is not a space integrated variable like *SP* or *CGP*. It does not depend upon or "feel" the entire field but rather samples a very small subset of it. The temporal variation of σ_{PD} is explained as follows. Systems that are more conducive to finger growth,

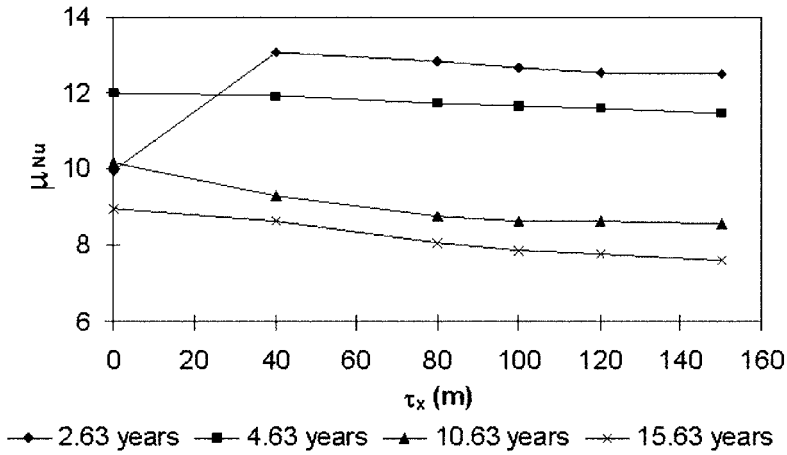

(a)

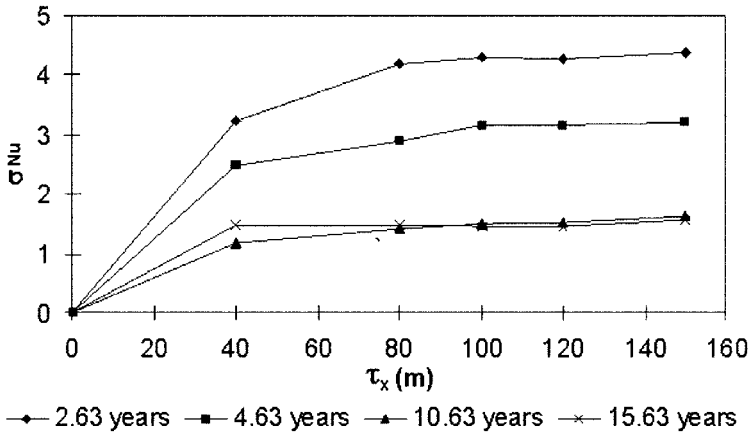

(b)

Figure 14. Variation of (a) the mean of the Nusselt number μ_{Nu} and (b) the standard deviation of the Nusselt number σ_{Nu} with horizontal correlation length (of log k) τ_x for different elapsed times. Note that homogeneous results are presented for comparison and are indicated by $\tau_x = 0$.

will experience larger growth of isolated fingers than systems which are less conducive. With increasing time, the contrast among responses of individual realizations increases. This is why a peak in σ_{PD} is observed. After that time, when the most conducive realization in any set has reached its maximum *PD* value, progressively more realizations will approach similar values. This reduces differences among responses of individual realizations and thus σ_{PD} reduces with time. The larger σ_y is, the more effective preferential flow paths become. This reduces the time for fingers to reach a certain-depth. Therefore, it is found that the maximum σ_{PD} occurs earlier for a highly heterogeneous system when compared to less heterogeneous ones. The reason for a decrease in σ_{PD} after it reaches a maximum is that after the time when the most conducive realization in any set has reached its maximum *PD* value, progressively more and more realizations will approach similar values.

3.3. Effect of τ_x on Output Variables

[36] For the sake of brevity we discuss the effect of τ_x on only one output variable, *Nu*. For the effect of τ_x on other variables, we will combine the discussion at the end of this section without giving their individual results since similar descriptions apply to all.

3.3.1. Nusselt Number (Nu)

[37] It is observed from the μ_{Nu} versus τ_x graph in Figure 14a that as τ_x increases μ_{Nu} decreases for all time. The decrease in μ_{Nu} implies a reduction in the degree of

instability. Therefore, an increase in τ_x appears to promote stability. Similar conclusions were reached by *Schincariol et al.* [1997]. An increase in τ_x implies longer and more continuous zones of high and low permeability. With a larger τ_x, lower permeability zones are more effective in dampening the upward and downward motions associated with a convecting fluid, both of which are necessary to promote and maintain the growth of instability. Therefore, an increase in τ_x causes a reduction in the degree of instability (albeit very small). Another possible reason for the decrease in the degree of instability with larger τ_x may be related to the likelihood of the dense plume ''seeing'' high- or low-permeability zones at the upper boundary. If τ_x is smaller, the probability of the top boundary interacting with a higher permeability zone is more than when τ_x is larger. It should, however, be noted that μ_{Nu} is not very sensitive to τ_x. An increase in τ_x from 40 m to 150 m (an increase of 270%) causes a maximum decrease in μ_{Nu} by just 11.8% at 20 years and much less than this at earlier times.

[38] The variation of σ_{Nu} with τ_x in Figure 14b shows that an increase in τ_x causes an increase in σ_{Nu}. The rate of increase of σ_{Nu} with respect to τ_x is higher at earlier times than at later times. This is due to the probability of the dense plume ''seeing'' a high- or low-permeability zone near the top boundary. For larger τ_x one might imagine either a laterally extensive sand or clay layer underlying most of the dense plume source. This results in either very unstable or weakly unstable to stable plumes in different realizations at earlier times. Resultant *Nu* therefore tend to differ more, which results in a correspondingly higher σ_{Nu}. With smaller τ_x, a combination of high- and low-permeability zones is more likely to intersect the top solute source boundary and individual realizations tend to be similar in their *Nu* responses. Thus a decrease in σ_{Nu} results with a reduction in τ_x. Due to stabilization of all systems at later times, irrespective of the magnitude of τ_x, *Nu* responses of different realizations decrease. Therefore the rate of increase of σ_{Nu} with respect to τ_x is retarded.

3.3.2. Effect of τ_x on the Other Indicator Variables

[39] A slight degree of reduction in the extent of fingering was observed from the mean concentration plots with increasing τ_x. However, the mean and the standard deviation of the concentration distribution were relatively insensitive to changes in correlation length. Results were difficult to interpret visually since the mean and the standard deviation profiles of concentration distribution corresponding to two consecutive values of τ_x appeared very similar. The difficulty in visually interpreting effects of changes in τ_x on the mean and standard deviation of concentration distribution justifies the need for use of variables like *SP* and *CGP* which can be interpreted quantitatively.

[40] An increase in τ_x caused a decrease in μ_{SP} at earlier times and caused an increase in μ_{SP} at later times. However, neither the initial decrease nor the later increase in μ_{SP} with τ_x was large. A change in τ_x from 40m to 150m (an increase of 275%) produced a maximum reduction of only 2% in μ_{SP} at 4.63 years simulation time and produced a maximum increase of only 7.34% at 20 years. The effect of an increase in μ_{SP} caused by increasing τ_x at later times is opposite to that seen in other variables. With the exception of *SP*, the magnitude of other indicator variables are largely determined by conditions near the top boundary alone. *SP* is determined by both upper and lower boundary conditions. One possible explanation for this behavior may be that an increase in τ_x causes an increase in the mass build up at later times by a net reduction in mass outflow from the bottom boundary. The increase in τ_x causes instabilities to be dampened and a reduction in solute mass leaving the system through the bottom boundary since a smaller number of plumes reach the bottom at later times. Although the mass influx at the source may itself be reduced with an increase in τ_x, the mass leaving the system through the bottom boundary may be reduced to a greater degree (concentration gradients driving diffusion through the bottom boundary are lower than that at the top; flux magnitudes at the bottom boundary are always notably lower than at the top boundary).

[41] An increase in τ_x caused an increase in σ_{SP} for all time which is expected because an increase in τ_x implies greater variability in individual responses of realizations due to greater contrasts among them as explained earlier. An increase in τ_x caused a decrease in μ_{CGP}, again consistent with its stabilizing effect. An increase in τ_x caused an increase in σ_{CGP} at earlier times, but had little effect at later times. An increase in σ_{CGP} with an increase in τ_x is expected because an increase in τ_x implies greater variability in individual responses of realizations due to greater contrasts among them which is more significant at earlier times than at later times.

[42] An increase in τ_x reduced μ_{PD} for all time again consistent with stabilization of solute transport processes. However, μ_{PD} was not very sensitive to the changes in τ_x. A 275 % increase in τ_x (from 40 m to 150 m) produced a maximum reduction of 11.75% at about one year. An increase in τ_x caused a general increase in σ_{PD}. However, the maximum overall increase in σ_{PD} was 34.2% at 8.63 years simulation time when τ_x increased from 40 m to 150 m (a 275% increase). An interesting observation was the maxima in σ_{PD} curves at $\tau_x \sim 100$ m at later times (greater than about 11 years). This may be related to the ratio of τ_x to the length of top solute source boundary but clearly warrants further investigation.

3.4. Effect of μ_y on Output Variables

[43] Due to qualitative similarities in the results and their causes, only a typical result showing the effect of μ_y on both μ_{PD} and σ_{PD} is given (Figure 15). This and other results showed that as μ_y increased there was virtually no change in the mean and standard deviations of output variables until a critical value of about $\mu_y \sim -13.3$ was reached. For values of μ_y higher than this apparent critical value, there was a rapid increase in the mean and standard deviations of all output variables. The lower (subcritical) μ_y appears to be consistent with diffusive/dispersive transport and the general absence of instability. Changing permeability (μ_y) in this stable range has little effect on the diffusive/dispersive transport. A rapid increase in the mean and standard deviations of output variables beyond the critical value for μ_y is consistent with the onset of instability as free convection then becomes the dominant mode of solute transport.

[44] It is useful to comment on the critical value of μ_y (~ -13.3). Although there is clearly a range over which transition from stable to unstable behavior appears to occur, it is interesting to note that this critical μ_y is equivalent to

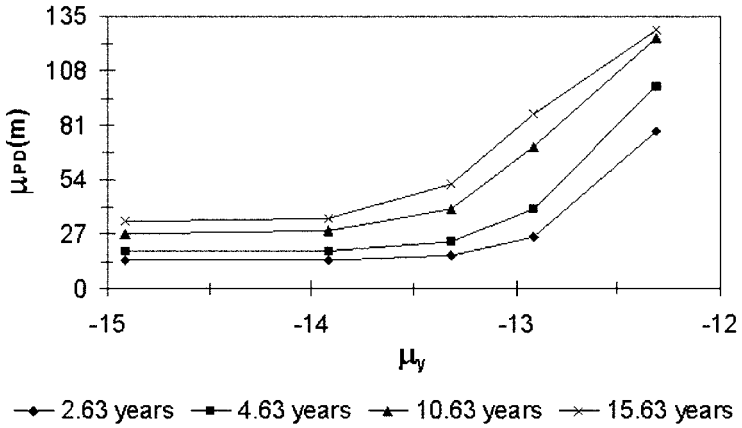

(a)

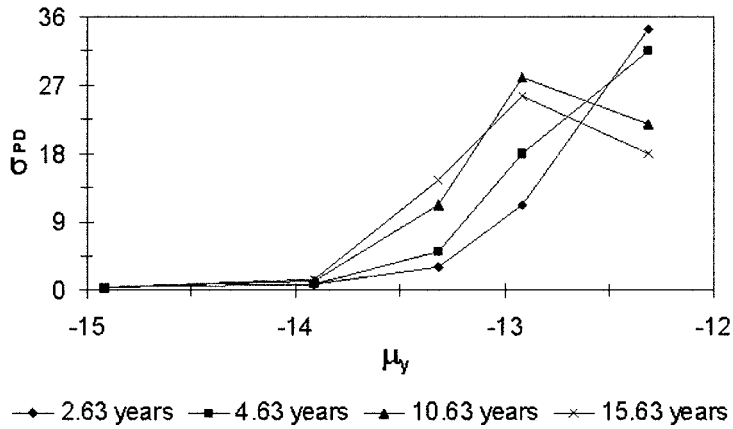

(b)

Figure 15. Variation of (a) the mean of the penetration depth (of 0.6 contour) μ_{PD} and (b) the standard deviation of the penetration depth with the mean (of log k) μ_y for different elapsed times.

the average permeability of 4.8×10^{-14} m^2 corresponding to a notional Rayleigh number, $Ra_{AV} = 40$. This Rayleigh number is identical to the critical Rayleigh number documented for the homogeneous case [*Elder*, 1967a]. This gives the impression that the onset of instability can be predicted by the Ra_{AV} (based upon the average permeability). However, it is clear that the high degree of uncertainty associated with the output variables restricts the usefulness of Ra_{AV} as a predictor of instability in heterogeneous cases as will be discussed in the following section.

3.5. Rayleigh Number as a Predictor of Instability in Heterogeneous Systems

[45] This study has shown how heterogeneity (i.e., σ_y, τ_x) play an important role in controlling the growth and decay of instabilities. These results do not address a central issue of prediction of instability in heterogeneous systems. The issue of predictive validity of *Ra* in heterogeneous systems was addressed by conducting stochastic experiments at a lower than critical μ_y (~ -13.315; $Ra_{AV} \sim 40$) value of $\mu_y = -13.917$ ($Ra_{AV} \sim 10$) for different values of σ_y. For one arbitrarily selected simulation set *m4sd4* from this experiment with $\sigma_y = 1.2$, realizations showing the minimum and maximum values of *PD* at selected elapsed times were identified. Results clearly demonstrated that a high degree of heterogeneity is capable of triggering instability even at a subcritical μ_y (and therefore subcritical Ra_{AV}). Thus, given results presented so far, it is clear that the Rayleigh number based upon average permeability could not be expected to adequately predict the onset of instability in a heteroge-

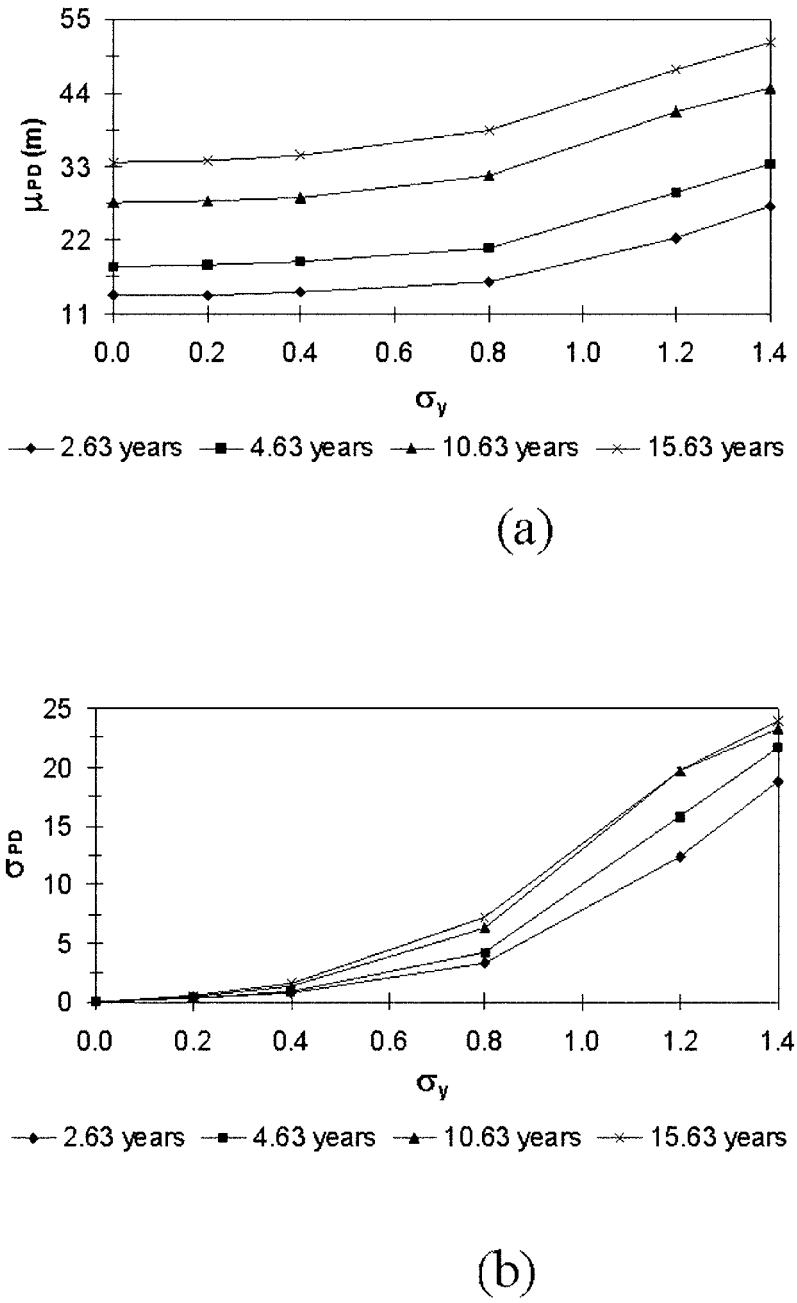

Figure 16. Variation of (a) the mean of the penetration depth (of 0.6 contour) μ_{PD} and (b) the standard deviation of the penetration depth (of 0.6 contour) σ_{PD} with the standard deviation (of log k with a lower mean) σ_y for different elapsed times.

neous system. Furthermore, it provides no information about the temporal development of instabilities once they are generated i.e., growth and/or decay rates which are clearly important in the analysis of the dense plume problem in heterogeneous porous media.

[46] A typical stochastic result showing the effect of σ_y (at a lower μ_y) on *PD* is shown in Figure 16. It is observed from this and other results (not given here) that as σ_y is increased, there is an increase in the mean and standard deviations of all output variables at all times. However, an increase in the mean and standard deviation are not significant unless σ_y reaches a critical value of about 0.8. Below this value of σ_y, the mean values of variables remain close to the homogeneous values. This is because most realizations are stable and the dominant mode of solute transport is diffusion. An increase in σ_y beyond 0.8 causes a significant increase in the mean values of variables. This occurs because some realizations even at this low μ_y ($Ra_{AV} = 10$) now become unstable, thereby increasing the mean values of variables. The onset of instability in some realizations causes increasing differences among responses of different realizations (with increasing σ_y), which leads to increasing standard deviations of output variables.

[47] It has been seen in the preceding section describing the effect of μ_y on the output variables that for a constant σ_y (0.4), there is a critical mean ($\mu_y \sim -13.315$; $Ra_{AV} \sim 40$)

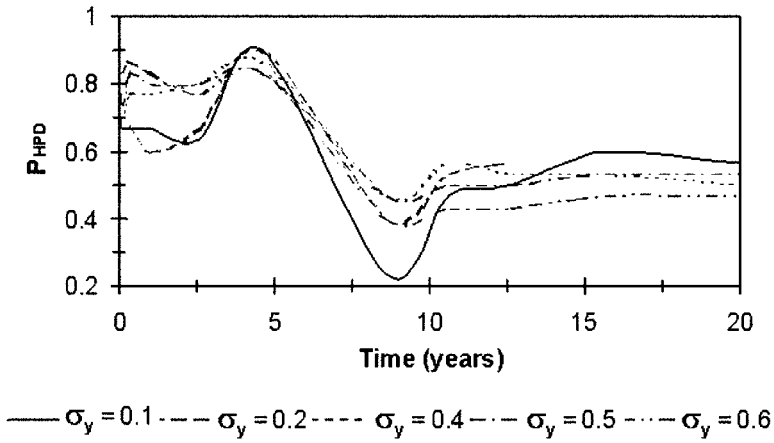

(a)

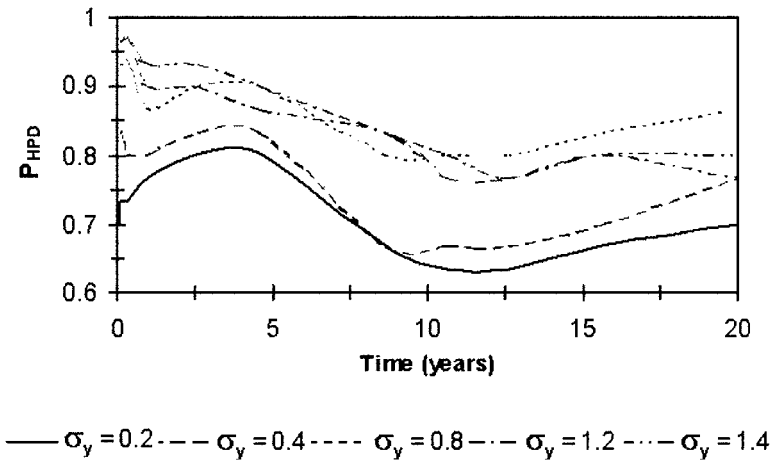

(b)

Figure 17. Variation of the probability of exceedence of the homogeneous penetration depth (of 0.6 contour) $\mathbf{P_{HPD}}$ with time for different values of standard deviation (of log k) σ_y for (a) a higher mean $\mu_y = -12.315$ and (b) a lower mean $\mu_y = -13.917$.

around which instability takes place. Here it is seen that for a constant subcritical mean ($\mu_y = -13.917$; $Ra_{AV} \sim 10$) there is a certain critical value of heterogeneity ($\sigma_y \sim 0.8$) around which instability can take place. These results together lead to a hypothesis that every value of μ_y may have an associated critical σ_y, at which instability can take place and vice versa. The upper bound for the critical μ_y occurs when σ_y is zero. Simply, this is to say that it is possible to observe instability at a less than critical mean permeability (critical *Ra* for homogeneous case), provided that there is a sufficient amount of heterogeneity present in the system.

3.6. Risk Analysis: The Probability of Exceedence Caused by Homogeneous Assumptions

[48] Risks are best described by the probability of exceedence of a particular value of an output variable of interest, given a certain degree of uncertainty in input parameters. The value of the probability of exceedence of *Nu* and *PD* were calculated relative to the corresponding homogenous case value of the variable. In other words, if we were to use a homogeneous model with equivalent average permeability, what is the likelihood we would underestimate an output variable such as *PD* or *Nu*? This helps to understand the implications of making an assumption about homogeneous conditions applying when heterogeneous conditions actually exist.

[49] The temporal variation of probability of exceedence of *PD*, $\mathbf{P_{HPD}}$ for different values of σ_y at higher $\mu_y = -12.315$ ($Ra_{AV} = 400$) and lower $\mu_y = -13.917$ ($Ra_{AV} = 10$) are given in Figures 17a and 17b. Although the temporal variation of $\mathbf{P_{HPD}}$ is complex, there are some clear trends in $\mathbf{P_{HPD}}$ with time both at higher and lower μ_y. In case of the higher μ_y, $\mathbf{P_{HPD}}$ is generally a maximum at elapsed times

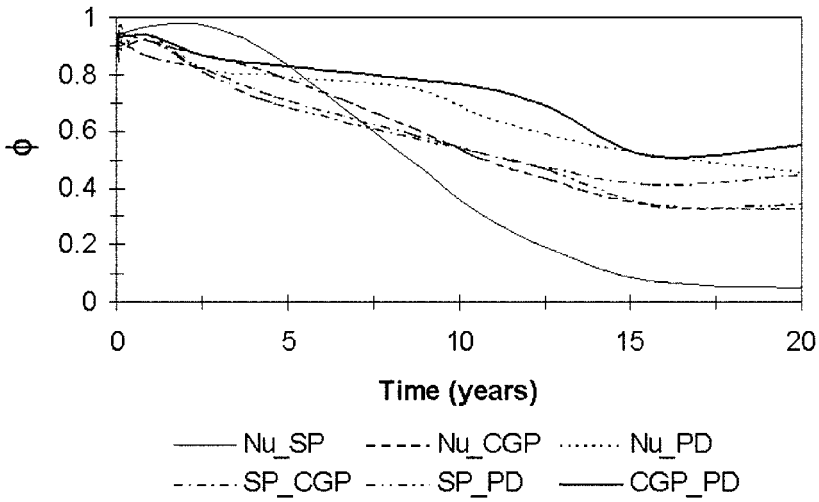

Figure 18. Calculated correlation coefficient ϕ versus time for each of the coupled pairs. Permeability field statistical parameters are $\mu_y = -12.315$; $\sigma_y = 0.6$; $\tau_x = 100$ m and *anis* 0.3

less than about 5 years and a minimum at around 9 years. $\mathbf{P_{HPD}}$ increases with time after about 9 years and stabilizes around 13 years. This is consistent with earlier observations of variations of these variables. Instabilities increase initially with time. At around 5 years instabilities are at a maximum. Therefore, this is the time interval around which a larger number of heterogeneous realizations have higher values of *PD* than in the homogeneous case. Gradually the degree of instability decreases. By around 9 years, highly unstable realizations begin to stabilize but this is also true of the homogeneous system. This brings the homogeneous behavior and the behavior of most heterogeneous realizations closer and therefore $\mathbf{P_{HPD}}$ is a minimum at about this time. In the heterogeneous case there may be late starters (initially not so conducive realizations), which may progressively become moderately to highly unstable beyond about 9 years in increasing numbers. *PD* in the homogeneous case also reduces slightly due to accumulation of mass in fingers. These cause $\mathbf{P_{HPD}}$ to increase. However, by about 13 years there are no new late starters and it is likely that those that can move faster than in the homogeneous equivalent are already doing so. This causes $\mathbf{P_{HPD}}$ to stabilize.

[50] For lower μ_y, $\mathbf{P_{HPD}}$ is a maximum at earlier times and continuously decreases for all values of σ_y. While the homogeneous case is fully stable, in many heterogeneous realizations fingers, however small, may initially grow. The number of heterogeneous realizations, where *PD* is higher than the homogeneous case, may be higher initially as heterogeneity promotes instability at early times. With time, in many realizations initial fingers may die out by diffusion/dispersion and thus $\mathbf{P_{HPD}}$ decreases with time. However, at later times (greater than about 13 years) some more conducive realizations may start showing unstable behavior after the accumulation of a sufficiently dense brine layer near the upper boundary. This again increases $\mathbf{P_{HPD}}$.

[51] It follows from the results presented in Figure 17 that we are likely to underestimate *PD* in 80 to 95% of cases at earlier times (less than about 5 years) and in 20 to 50% cases at later times (greater than about 9 years) at a higher mean. For a lower (subcritical) mean, *PD* is underestimated in 70 to 97% cases at earlier times and in 70 to 87% cases at later times. Risks are considerably high in the case of systems expected to be unstable as predicted by a mean permeability ($Ra_{AV} = 400$), but even higher in supposedly stable systems as predicted by a mean permeability ($Ra_{AV} = 10$). Results clearly show that the risk involved in the case of a low-permeability field with a higher degree of heterogeneity (σ_y) is greater than the risk associated with a high-permeability field with a lower degree of heterogeneity (σ_y).

3.7. Correlation Between Output Variables

[52] The interrelationship between different output variables was investigated by determining correlation coefficients between output variable pairs. These are denoted by (1) Nu_SP, (2) Nu_CGP, (3) Nu_PD, (4) SP_CGP, (5) SP_PD and (6) CGP_PD. Figure 18 gives the calculated correlation coefficient versus time for each of the coupled pairs for simulation set *rg3sd4* ($\mu_y = -12.315$; $\sigma_y = 0.6$; $\tau_x = 100$ m and *anis* = 0.3). It is apparent that (1) all correlation coefficients are positive at all times, i.e., output variables are positively correlated for all time and for all values of input variables and (2) the magnitude of correlation coefficients are not constant with time. At earlier times, all correlation coefficients are very high (≥ 0.8) but decrease with time with the lowest correlation observed at later times between *Nu* and *SP*. This implies that except for at early times, one output variable cannot be determined from knowledge of another with a high degree of confidence. This serves as additional justification for the use of a number of indicator variables, especially in light of the transient nature of the processes under consideration.

4. Summary and Conclusions

[53] It is clear from the results of this study that heterogeneity plays two mutually opposing time-dependent roles in controlling convective instabilities. It serves as the triggering mechanism and therefore promotes instabilities at early times but tends to dissipate them at later times by enhancing dispersive mixing. A visual examination of dense

plume behavior in statistically equivalent permeability fields showed that dense plume migration rates and pathways were significantly different and that a stochastic analysis of a larger number of realizations was warranted. A number of quantitative indicators were employed to analyze the outputs including concentration distributions, Nusselt numbers, solute present in the system, center of gravity of plume and penetration depth of fingers.

[54] The main conclusions from the study are the following.

1. An increase in the standard deviation of the log permeability field causes an increase in the degree of instability at earlier times but promotes stability at later times.

2. An increase in the horizontal correlation length of the log permeability field (creates laterally extensive low-permeability zones that dissipate upward and downward motions needed to maintain convection) causes a decrease in the degree of instability at all times, as indicated by a reduction in mean values of output variables. However, in comparison to the effect of mean and standard deviation of the log permeability field, processes appear relatively insensitive to correlation length of the distribution.

3. An increase in the mean of the log permeability field causes an increase in the degree of instability at all times, as shown by a consistent increase in the mean values of output variables.

4. Increasing the standard deviation, correlation length and the mean of the log permeability field cause an increase in the degree of uncertainty of predictions as indicated by the higher standard deviation of output variables. The temporal trends in the standard deviations of the different output variables are complex.

5. The traditional Rayleigh stability criterion based upon an average permeability is inadequate for describing solute transport processes in heterogeneous systems. Results show that instability can occur at a subcritical mean of the log permeability field (and hence subcritical Rayleigh number) where sufficient heterogeneity associated with larger field standard deviation exists.

6. Probability of exceedence analysis has shown that analyses based upon homogeneous assumptions will typically underestimate, often significantly, the value of key output variables where heterogeneous conditions actually exist. This has significant implications for modeling and prediction of dense plume pathways and migration rates in heterogeneous porous media.

7. Correlation coefficients between output indicators were positive at all times. The magnitude of these coefficients were, however, seen to be time dependent. At earlier times, all correlation coefficients were very high ($\geq$0.8). All correlation coefficients decreased with time, with the lowest correlation at later times observed between *Nu* and *SP*. This serves as additional justification for the use of a number of indicator variables, especially in light of the transient nature of the processes under consideration.

[55] While general "cause and effect" trends are clear from the results of this study, problems still exist. The precise nature of the quantitative relationship between instability onset, as well as subsequent growth or decay, and the nature of heterogeneity (e.g., magnitude, geometry) requires elucidation. Although the results of our study agree with the results of *Schincariol et al.* [1997], other system geometries and boundary conditions could be studied to determine whether these results are indeed generalizable. Furthermore, difficulties remain as to how to predict the migration rates and pathways of a dense contaminant plume in field settings, where heterogeneity may not be adequately quantifiable. A stochastic analysis may permit boundaries on the likely range of behavior to be determined but prediction of more precise rates and pathways consistent with the single field realization is currently not possible. Other questions remain in order to address these issues and include: at what scale must we resolve heterogeneity in field settings to adequately predict and model solute transport processes? What level of simplification in the detail of heterogeneity is permissible before we no longer model the real system? How do we incorporate key characteristics of the heterogeneous permeability field into predictive stability criteria? These are just some unanswered questions that warrant further investigation.

Notation

ΔC concentration difference as mass fraction between source (upper) and sink (lower) boundaries (MM^{-1}).

$\boldsymbol{\tau_x}$ horizontal correlation length (L).

$\boldsymbol{\tau_y}$ vertical correlation length (L).

$\boldsymbol{\sigma_y}$ standard deviation of the random variable Y (L^2).

$\nu_0 = \mu/\rho_0$ kinematic viscosity of the fluid (L^2T^{-1}).

$anis = \boldsymbol{\tau_y/\tau_x}$ ratio of vertical length to horizontal correlation length

C fluid concentration expressed as a mass fraction (MM^{-1}).

CGP center of gravity of the plume at a particular time (L).

D_o apparent molecular diffusivity of solutes in a porous medium (L^2T^{-1}).

g acceleration due to gravity (LT^{-2}).

H depth of the porous layer or model domain (L).

k intrinsic permeability (L^2).

L_s length of the source boundary (L).

MC number of Monte Carlo simulations.

Nu Nusselt number at a particular time (dimensionless).

$\mathbf{P}$ probability of exceedence of the value of a variable in case of the corresponding homogeneous system at a particular time (dimensionless).

PD penetration depth of 0.6 concentration contour at a particular time (L).

$\mathbf{P_{HPD}}$ probability of exceedence of the variable PD (dimensionless).

Q solute flux rate (MT^{-1}).

Ra is the Rayleigh number of solutes (dimensionless).

Ra_{AV} is the average Rayleigh number for a heterogeneous system.

SP is a quantity proportional to the amount of solute present in the aquifer at a particular time (L).

T time (T).

W width of the source boundary (L).

X, Y, Z axes names in a Cartesian coordinate system.

x, y, z spatial coordinates (L).

$\mathbf{Y}$ random variable and equals log of the permeability, k (L^2).

Δx horizontal length of a finite element or cell (L).

Δy is the vertical length of a finite element or cell (L).

$\Delta\rho$ density contrast between the solute source and the underlying groundwater (ML^{-3}).

α_T transverse dispersivity of the porous medium (L).

$\beta = \rho_0^{-1}(\partial\rho/\partial C)$ coefficient of density variability (dimensionless).

ε porosity (dimensionless).

μ fluid dynamic viscosity ($M(LT)^{-1}$).

$\boldsymbol{\mu_{CGP}}$ mean of the variable *CGP* at a particular time (L).

$\boldsymbol{\mu_{Nu}}$ mean of the Nusselt number at a particular time (dimensionless).

$\boldsymbol{\mu_{PD}}$ mean of the variable *PD* at a particular time (L).

$\boldsymbol{\mu_{SP}}$ mean of the variable *SP* at a particular time (L).

$\boldsymbol{\mu_y}$ mean of the random variable Y = log k (L^2).

ρ fluid density (ML^{-3}).

ρ_o fluid density (ML^{-3}) at base concentration C_o ($M_S M^{-1}$).

$\boldsymbol{\sigma_{CGP}}$ standard deviation of the variable *CGP* (L).

$\boldsymbol{\sigma_{Nu}}$ standard deviation of the Nusselt number (dimensionless).

$\boldsymbol{\sigma_{PD}}$ standard deviation of the variable *PD* (L).

$\boldsymbol{\sigma_{SP}}$ standard deviation of the variable *SP* (L).

[56] **Acknowledgments.** The study was conducted with supporting Postgraduate scholarships from the Flinders University of South Australia and Center for Groundwater Studies, Australia for Awadhesh Prasad. The authors gratefully acknowledge conversations with Clifford Voss about the SUTRA model and with Robin A. Wooding about instability theory. Robert Schincariol and Ward Sanford provided extensive comments on the thesis from which the material in this paper is derived. We thank Douglas Weatherill who provided comments on an earlier draft of the manuscript. The authors gratefully acknowledge reviews by Mike Nicholl and Zhi Wang whose comments helped to greatly improve the manuscript.

References

Deutsch, C. V., and A. G. Journel, *GSLIB Geostatistical Software Library and Users Guide*, Oxford Univ. Press, New York, 1992.

Elder, J. W., Steady free convection in a porous medium heated from below, *J. Fluid Mech.*, *27*(1), 29–48, 1967a.

Elder, J. W., Transient convection in a porous medium, *J. Fluid Mech.*, *27*(3), 609–623, 1967b.

Frind, E. O., Simulation of long term density-dependent transport in groundwater, *Adv. Water Resour.*, *5*, 73–97, 1982.

Gebhart, B., Y. Jaluria, R. L. Mahajan, and B. Sammakia, *Buoyancy-Induced Flows and Transport*, Taylor and Francis, Philadelphia, Pa., 1988.

Huyakorn, P. S., P. F. Andersen, J. W. Mercer, and H. O. White, Saltwater intrusion in aquifers: Development and testing of a three-dimensional finite element model, *Water Resour. Res.*, *23*(2), 293–312, 1987.

Kolditz, O., R. Rathke, H.-J. Diersch, and W. Zielke, Coupled groundwater flow and transport, 1, Verification of variable density flow and transport models, *Adv. Water Res.*, *21*(1), 27–46, 1998.

Kreyszig, E., *Advanced Engineering Mathematics*, 6th ed., John Wiley, New York, 1988.

Moissis, D. E., and M. F. Wheeler, Effect of the structure of the porous medium on unstable miscible displacement, in *Dynamics of Fluids in Hierarchical Porous Media*, edited by J. H. Cushman, pp 243–271, Academic, San Diego, Calif., 1990.

Mulqueen, J., and D. Kirkham, Leaching of a surface layer of sodium chloride into tile drains in a sand-tank model, *Soil. Sci. Soc. Am. J.*, *36*, 3–9, 1972.

Nield, D. A., and A. Bejan, *Convection in Porous Media*, Springer-Verlag, New York, 1999.

Oldenburg, C. M., and K. Pruess, Dispersive transport dynamics in a strongly coupled groundwater-brine flow system, *Water Resour. Res.*, *31*(2), 289–302, 1995.

Schincariol, R. A., Dispersive mixing dynamics of dense miscible plumes: Natural perturbation initiation by local-scale heterogeneities, *J. Contam. Hydrol.*, *34*, 247–271, 1998.

Schincariol, R. A., and F. W. Schwartz, An experimental investigation of variable density flow and mixing in homogeneous and heterogeneous media, *Water Resour. Res.*, *26*(10), 2317–2329, 1990.

Schincariol, R. A., F. W. Schwartz, and C. A. Mendoza, Instabilities in variable density flows: Stability and sensitivity analyses for homogeneous and heterogeneous media, *Water Resour. Res.*, *33*(1), 31–41, 1997.

Schincariol, R. A., F. W. Schwartz, and C. A. Mendoza, On the generation of instabilities in variable density flow, *Water Resour. Res.*, *30*(4), 913–927, 1994.

Simmons, C. T., and K. A. Narayan, Mixed convection processes below a saline disposal basin, *J. Hydrol.*, *194*, 263–285, 1997.

Simmons, C. T., and K. A. Narayan, Modelling density-dependent flow and solute transport at the Lake Tutchewop saline disposal complex, Victoria, *J. Hydrol.*, *206*, 219–236, 1998.

Simmons, C. T., K. A. Narayan, and R. A. Wooding, On a test case for density-dependent groundwater flow and solute transport models: The Salt Lake problem, *Water Resour. Res.*, *35*(12), 3607–3620, 1999.

Simmons, C. T., T. R. Fenstemaker, and J. M. Sharp Jr., Variable-density groundwater flow and solute transport in heterogeneous porous media: Approaches, Resolutions and Future Challenges, *J. Contam. Hydrol.*, *52*(1–4), 245–275, 2001.

Valliappan, S., W. Wang, and N. Khalili, Contaminant transport under variable density flow in fractured porous media, *Int. J. Numer. Anal. Meth. Geomech.*, *22*, 575–595, 1998.

Voss, C. I., SUTRA: A finite-element simulation model for saturated-unsaturated fluid density-dependent groundwater flow with energy transport or chemically reactive single-species solute transport, *U.S. Geol. Surv. Water Resour. Invest. Rep., 84–4369*, 409 pp., 1984.

Voss, C. I., and W. R. Souza, Variable density flow and solute transport simulation of regional aquifers containing a narrow freshwater-saltwater transition zone, *Water Resour. Res.*, *23*(10), 1851–1866, 1987.

Wooding, R. A., S. W. Tyler, and I. White, Convection in groundwater below an evaporating salt lake, 1, Onset of instability, *Water Resour. Res.*, *33*(6), 1199–1217, 1997a.

Wooding, R. A., S. W. Tyler, I. White, and P. A. Anderson, Convection in groundwater below an evaporating salt lake, 2, Evolution of fingers or plumes, *Water Resour. Res.*, *33*(6), 1219–1228, 1997b.

A. Prasad and C. T. Simmons, School of Chemistry, Physics and Earth Sciences, Flinders University of South Australia, GPO Box 2100, Adelaide, South Australia 5001, Australia. (craig.simmons@flinders.edu.au)